

# An Analysis of the Sediment Transport Characteristics in the Aur River

**Muhammad Amin**

Civil Engineering Department, Faculty of Engineering, Hasanuddin University, Gowa, Indonesia  
amin.construct@gmail.com (corresponding author)

**Muhammad Saleh Pallu**

Civil Engineering Department, Faculty of Engineering, Hasanuddin University, Gowa, Indonesia  
salehpallu@hotmail.com

**Farouk Maricar**

Civil Engineering Department, Faculty of Engineering, Hasanuddin University, Gowa, Indonesia  
faroukmaricar@unhas.ac.id

**Rita Tahir Lopa**

Civil Engineering Department, Faculty of Engineering, Hasanuddin University, Gowa, Indonesia  
ritalopa04@yahoo.com

Received: 14 January 2026 | Revised: 5 March 2026 and 29 March 2026 | Accepted: 1 April 2026

Licensed under a CC-BY 4.0 license | Copyright (c) by the authors | DOI: <https://doi.org/10.48084/etasr.17536>

## ABSTRACT

Studies on river sediment characteristics have evolved, particularly regarding the interaction between hydrological dynamics and sediment transport. Based on hydraulic and sedimentological analysis, the Aur River is in an active morphodynamic condition with a flow transport capacity that significantly exceeds the sediment mobilization threshold, both for fine ( $D_{50}$ ) and coarse ( $D_{90}$ ) fractions. The very large value of the ratio of shear stress to critical stress ( $\tau/\tau_c$ ) indicates that the river system is over-competent, so that fine sediment is always in suspension and coarse sediment is very easily transported as bed load. The longitudinal distribution shows a pattern of degradation in the upstream section, dominant transport in the middle section, and a tendency towards aggradation in the downstream section. The non-proportional increase in the discharge-concentration relationship indicates that this system operates in a supply-limited regime, where transport capacity exceeds the available sediment supply. Thus, the long-term stability of the river depends primarily on changes in sediment supply from the catchment area rather than on variations in flow energy alone.

*Keywords-sediment; river; bed load; degradation*

## I. INTRODUCTION

Studies on hydrological dynamics and sediment transport in rivers usually follow three main approaches: the hydrodynamic and sediment transport approach, the grain size distribution and deposition analysis approach, and the seasonal and climate variability approach to sediment load. Changes in hydraulic conditions due to floodgate adjustments directly impact sediment transport distribution and patterns. The important relationship between flow velocity, shear stress, and sediment transport capacity has been emphasized [1]. The development of a non-uniform sediment transport model highlights the role of grain size distribution in determining flow resistance and alluvial riverbed stability. This model is widely used in the analysis of sandy and gravel rivers [2]. However, most studies

are model-based or conducted in non-tropical rivers; thus, empirical validation in tropical regions remains limited.

Sediment transport rates in tropical rivers are significantly influenced by seasonal changes [3]. Extreme climate conditions can drastically alter sediment load patterns, especially in large rivers [4]. Sediment deposition is closely related to the stability of riverbank morphology [5]. However, research has mainly focused on large-scale rivers or delta systems, so the characteristics of local-scale tropical rivers have not been thoroughly investigated. Sediment characteristics in upstreams of tropical rivers are based on grain-size distribution [6]. Geochemical approaches have also been used to understand estuarine sedimentation trends [7]. It has been further shown that bed load and suspended load are often analyzed separately [8-10]. Thus, previous studies have failed to integrate both bed

and suspended sediment analysis within a single tropical river system using comprehensive field hydrodynamic data.

Based on the literature review, there is a lack of empirical studies based on field data on local-scale tropical rivers. Furthermore, bed and suspended sediment have not been analyzed in an integrated hydrodynamic framework. The quantitative relationship between rainy season flow velocity and sediment grain size distribution in tropical river systems has been minimally tested. Finally, there is an absence of location-specific characterization that connects geomorphological maps with actual sediment transport dynamics.

## II. MATERIALS AND METHODS

### A. Location and Time

The research was conducted on the Aur River in 2024. Observation points represented the upstream, midstream, and downstream conditions of the river. The sampling points were determined based on the accessibility of the location by vehicles, both by land and by river. The field conditions were safe for sampling. The currents were not extreme, and the cliffs were not steep, making it easy to carry sampling equipment. Overall, the research location was safe and practical for measurement. Furthermore, the Aur River has variations in its morphology. At the estuary, the river flow is straight, in the middle section it meanders, and then at the bottom the river flow is straight again. The Aur River, in the center of Palembang City, is located in 9/10 Ulu Village, Jakabaring District. The research location can be seen in Figure 1.

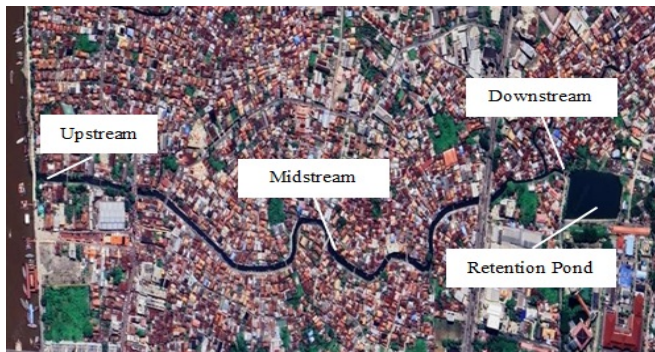


Fig. 1. Research location.

### B. Data Types

The primary data collected in the field include topographic data, bed sediment data, suspended sediment data, and grain size data from sieve analysis ( $D_{50}$  and  $D_{90}$ ). Secondary data were obtained from other sources, such as satellite imagery.

### C. Data Collection Methods

Topographic measurements were conducted from the estuary to the bottom of the river using survey instruments. Measurements were taken both transversely and longitudinally, and included river width, depth, elevation, and slope. The cross-section of the segments of the river is illustrated in Figure 2.

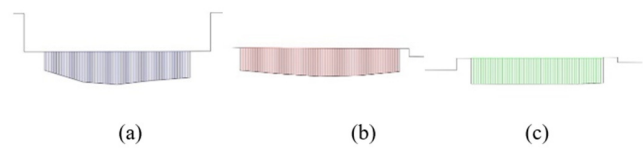


Fig. 2. Cross-section: (a) upstream, (b) midstream, (c) downstream

Bottom sediment data were collected using a grab sampler, and floating sediment data were collected using a Van Dorn Water Sampler. The procedure for both tools involves identifying the river segment, namely the estuary-middle-downstream, and determining the sampling location and the number of sample points. Then, the river width is divided into 3 parts: left, middle, and right. Bottom sediment samples are taken from each one of them. Before being placed at each point, the grab sampler is in an open position. It is then placed on the bottom of the river, where a weight is released so that both sides of the tool are closed. Finally, the bottom sediment that has been captured in the tool is lifted. Floating sediment samples are also taken in each part of the river, and both types of samples are then put into plastic bags for analysis in the soil laboratory. Furthermore, a current meter is used to measure the flow velocity, placing it at depths of 0.2h, 0.6h, and 0.8h of the river water. For river depths below 1.5 m, 0.6h is used.

### D. Data Analysis Methods

Sieve analysis (grain size analysis) was carried out to determine the distribution of basic sediment grain sizes. Samples that have been taken using the grab sampler are first dried and then weighed, before being put through a set of standard sieves, ranging from large to small diameters, using a sieve shaker for 10-15 min. The sediment retained on each sieve is subsequently weighed. From the results of the grain size distribution analysis, the  $D_{50}$  and  $D_{90}$  values are obtained.

Suspended sediment analysis is conducted using the filtration method. For this, the water is placed into a measuring cup, recording its volume. A filter paper is used, which must be weighed while dry (W1). The sample water is filtered utilizing a vacuum pump until all sediment is retained. The filter paper is then put into an oven at a temperature of 105°C for approximately 24 h, and when it cools, it is placed in a desiccator. After this, the filter is weighed again (W2). The sediment concentration  $C_s$  (g/l), the flow discharge  $q_w$  (m<sup>3</sup>/s), and the sediment discharge  $q_s$  (tons/day) are calculated by:

$$C_s = \frac{W_s}{V_t} \quad (1)$$

$$\bar{V} = \frac{V_1 + V_2 + V_3}{3} \quad (2)$$

$$q_w = A \times \bar{V} \quad (3)$$

$$q_s = 0,0864 \times C_s \times q_w \quad (4)$$

where:

- $W_s$  = sediment weight (g)
- $V_t$  = sample volume of sediment and water (l)
- $\bar{V}$  = average water flow velocity (m/s) at observation points 1, 2, and 3

- $A$  = cross-sectional area ( $m^2$ )

The type of sediment transport was determined by comparing the grain size distribution ( $D_{50}$ ,  $D_{90}$ ) and the concentration of suspended sediment, as well as by calculating the ratio of bed load to suspended load. Riverbed stability was evaluated by analyzing the shear stress of the flow compared to the critical stress of grain movement. Erosion and deposition zones were identified from variations in sediment size, changes in flow velocity, and differences in upstream-downstream cross-sectional morphology. The integration of all these parameters was used to assess the dynamic trend of river morphology, whether it leads to degradation, aggradation, or a relatively stable condition. Bed sediment transport was calculated using:

$$\tau = \rho g R S \quad (5)$$

$$\tau_c = \theta_c (\rho_s - \rho) g D \quad (6)$$

where:

- $\tau$  = shear stress ( $N/m^2$ )
- $\rho$  = water density ( $kg/m^3$ )
- $g$  = gravitational acceleration ( $9.81 m/s^2$ )
- $R$  = hydraulic radius (m)
- $S$  = energy slope/river bed slope
- $\tau_c$  = critical shear stress ( $N/m^2$ )
- $\theta_c$  = critical shield parameter
- $\rho_s$  = sediment density ( $kg/m^3$ )
- $\rho$  = water density ( $kg/m^3$ )
- $D$  = grain diameter (m)

The  $D$  value used to calculate the critical shear stress is derived from the  $D_{50}$  or  $D_{90}$  grain sieve analysis.

### III. RESULTS AND DISCUSSION

Topographic measurements start from upstream to downstream. The total length of the channel is 1.425 m. The survey data in Table I suggest that in the upstream section, the greatest relative depth indicates strong flow energy and high vertical erosion potential, leading to dominant bed erosion compared to lateral sedimentation. In the midstream section, the greatest width indicates channel widening due to lateral erosion. The river depth is shallower than upstream because the flow energy begins to decrease. The meander pattern indicates that the river has entered a dynamic equilibrium phase dominated by lateral erosion and sedimentation on the inside of the bend. In the downstream section, the narrowing width is unusual for natural patterns; this condition is due to the large number of residential houses along the riverbank. The shallowest depth indicates low flow energy and a tendency for sedimentation. In general, the Aur River can be explained as having morphological differences influenced by the distribution of flow energy, erosion, and sedimentation processes, as well as by the surrounding topography.

TABLE I. TOPOGRAPHIC CHARACTERISTICS OF THE RIVER

Position	Width (m)	Depth (m)	Slope
Upstream	10.7	2.3	0.00089
Midstream	11.4	1.7	0.00089
Downstream	5.8	1.1	0.00089

Flow velocity measurements in the Aur River were conducted once during the rainy season. In the upstream and midstream parts, nine measurements were taken. The cross-section was divided into three sections: left, middle, and right. Each section was measured three times at depths of 0.2h, 0.6h, and 0.8h. In the downstream part, only one measurement was carried out on each section, because the water depth was only around 1 m. The average flow rate was then calculated from the measurement results, as depicted in Table II.

TABLE II. FLOW RATE RECAPITULATION

Position	Flow rate (m/s)						
	Upstream		Midstream		Downstream		
Depth	0.2	0.6	0.8	0.2	0.6	0.8	0.6
TP1	0.21	0.19	0.20	0.21	0.19	0.18	0.20
TP2	0.23	0.24	0.26	0.21	0.23	0.22	0.20
TP3	0.22	0.19	0.19	0.21	0.19	0.18	0.20

In the upstream section, the highest discharge ( $5.30 m^3/s$ ) indicates that the largest water supply is in this segment (Table III). With the highest flow rate of  $0.22 m/s$ , the flow energy is relatively greater. In addition, the river's relatively deep cross-section allows for stable flow. The straight channel conditions result in a more focused energy distribution towards the downstream direction (minimal energy loss due to bends). In the midstream section, the flow discharge decreases from  $5.30 m^3/s$  upstream to  $3.94 m^3/s$ . The flow rate is slightly lower ( $0.20 m/s$ ) than before. River bends result in energy loss due to friction and changes in flow direction. With a larger river width and shallower depth, the flow will spread out. In the downstream section, the smallest flow discharge is  $1.28 m^3/s$  due to a significant decrease from the upstream. The flow rate is the same as the midstream, but due to the smaller cross-section, the water volume is much less. The depth is shallower due to low sediment transport energy.

TABLE III. AVERAGE FLOW RATE AND DISCHARGE

Position	Average flow rate (m/s)	Average flow discharge ( $m^3/s$ )	Standard deviation
Upstream	0.22	5.30	0.0018
Midstream	0.20	3.94	0.0009
Downstream	0.20	1.28	0

The sieve analysis results indicate that the bottom sediment is dominated by silt. The laboratory test results are presented in Table IV.

TABLE IV. GRAIN SIZE ANALYSIS

Position	$D_{50}$ (mm)	$D_{90}$ (mm)	Type of sediment
Upstream	0.0156	0.4889	silt
Midstream	0.0196	0.3243	silt
Downstream	0.0201	0.3445	silt

Based on these data, it can be observed that in the upstream section,  $D_{50} = 0.0156$  mm is included in the fine silt category, and  $D_{90} = 0.4889$  mm is close to medium-coarse sand. Hydraulically, the upstream section has the highest energy and discharge. In theory, higher energy can transport coarser particles, but the dominance of silt indicates that the riverbed material is dominated by fine sediment. It is likely that the supply of fine sediment is high from the catchment area, and the velocity of 0.22 m/s is still relatively low for continuous transport of coarse sand. The coarse fraction ( $D_{90}$ ) is possibly only transported during peak discharge (flood). This indicates a very wide grain size distribution because there are very fine to relatively coarse fractions. In the midstream section,  $D_{50}$  is slightly larger than upstream; so, the silt is somewhat coarser.  $D_{90}$  decreases compared to upstream; thus, the very coarse fraction is smaller. The grain distribution is still wide, but more sorted than upstream. Hydraulically, the flow energy is smaller than upstream. In meander channels, erosion occurs on the outer side of the bend, while silt deposition occurs on the inner side. Grain size is relatively uniform due to the natural selection process of the meander flow. In the downstream section,  $D_{50}$  is at most 0.0201 mm, but remains in the silt category.  $D_{90}$  increases slightly compared to the midstream section but remains smaller than the upstream section. Hydraulically, the smallest discharge results in low transport energy. The dominance of fine sediment indicates that coarse particles have been deposited in the previous section, and the remaining material is silt, which is easily transported as a suspension. The dominant transport is suspended load, and sediment is relatively more uniform compared to the upstream section. The composition of sedimentary material for each segment is illustrated in Figure 3.

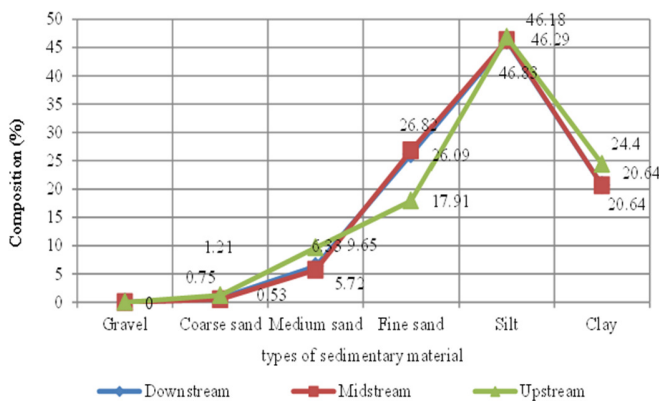


Fig. 3. Type of sedimentary material.

Shear stress ( $\tau$ ) is the shear force per unit area acting parallel to the riverbed due to water flow. Critical shear stress ( $\tau_c$ ) is the minimum value of shear stress required to start moving sediment particles from a state of rest. If  $\tau < \tau_c$ , then the sediment is still (stable). If  $\tau = \tau_c$ , then the sediment starts to move. If  $\tau > \tau_c$ , then the sediment is transported, and if  $\tau/\tau_c \gg 1$ , then sediment transport becomes intensive and there is potential for high degradation.

Table V shows that in the upstream section, the shear stress is significantly higher than the critical stress, in the case of  $D_{50}$

particles. This means that  $D_{50}$  particles (silt) are highly eroded and transported, making them unsteady on the riverbed.  $D_{50}$  is located deep within the erosion zone. Transport is predominantly in suspension. The riverbed is not controlled by  $D_{50}$ , but rather by coarser fractions. In the midstream section, shear stress is also very high.  $D_{50}$  remains mobile. The silt will not stabilize on the bed. Sedimentation only occurs when velocity drops drastically (inside meanders), and discharge decreases significantly. In the downstream section, theoretically,  $D_{50}$  remains mobile. However, in practice, the system energy is lower, discharge is small, and silt transport is highly dependent on momentary discharge. Sediment can form even when the flow slows even slightly. Overall,  $D_{50}$  (silt) never stabilizes as permanent bed sediment. The river is classified as suspended-load dominated. Bed material is likely controlled by coarser fractions. The high stress-to-stress ratio indicates that the system has much more energy than is required to move the silt. If sedimentation still occurs, it is due to local velocity reduction, channel widening, and calm water areas.

Table VI indicates that in the upstream section, the shear stress is greater than the critical stress for  $D_{90}$  particles as well. The coarse fraction is highly mobile. There is no permanent bed stability at this size. The riverbed is in a fully mobile bed condition. There is potential for bed scouring. During floods, total mobilization of the coarse fraction occurs. The upstream is a zone of very high energy for  $D_{90}$ . In the midstream section, although the absolute shear stress is lower,  $\tau_c$  is also lower; thus, it is relatively more mobile.  $D_{90}$  is very unstable. In the meander zone, strong erosion occurs on the outside of the bend. The midstream section is also in a condition of intensive transport for  $D_{90}$ . In the downstream, shear stress is almost 78 times the movement threshold, still far above the stable conditions. However, the energy is smaller compared to other segments. Mobility remains high, but the lowest in relative terms.  $D_{90}$  remains unstable, but the transport tendency is lower than upstream and midstream. The results for shear stress and critical shear stress for  $D_{90}$  are displayed in Figure 4.

TABLE V. BED SEDIMENT CHARACTERISTICS FOR  $D_{50}$

Position	Shear stress $\tau$ (N/m <sup>2</sup> )	Critical shear stress $\tau_c$ (N/m <sup>2</sup> )	Ratio $\tau/\tau_c$
Upstream	20.08	0.0067	2975.46
Midstream	14.84	0.0077	1927.44
Downstream	9.6	0.0072	1336.25

TABLE VI. BED SEDIMENT CHARACTERISTICS FOR  $D_{90}$

Position	Shear stress $\tau$ (N/m <sup>2</sup> )	Critical shear stress $\tau_c$ (N/m <sup>2</sup> )	Ratio $\tau/\tau_c$
Upstream	20.08	0.2115	94.94
Midstream	14.84	0.1274	116.49
Downstream	9.6	0.1232	77.96

The concentration of suspended sediment shows spatial variations influenced by flow velocity. High-velocity segments demonstrate increased concentrations of fine sediment. The characteristics of suspended sediment are presented in Table VII.

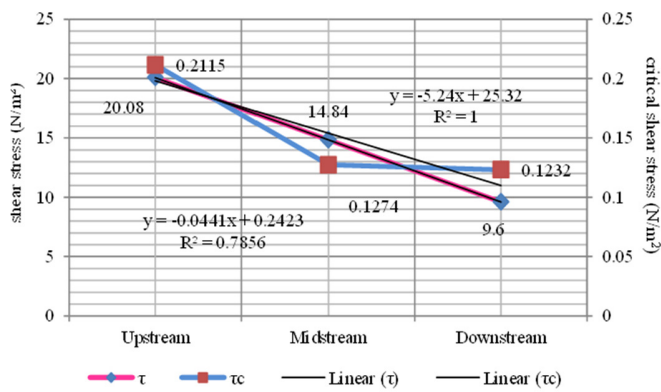


Fig. 4. Comparison of shear stress and critical shear stress.

TABLE VII. CHARACTERISTICS OF SUSPENDED SEDIMENT

Position	Average flow discharge $q_w$ (m <sup>3</sup> /s)	Average sediment concentration $C_s$ (g/l)	Average sediment discharge $q_s$ (tons/day)
Upstream	5.30	0.09	0.043
Midstream	3.94	0.07	0.023
Downstream	1.28	0.05	0.006

The upstream section has the highest discharge and concentration, the highest flow energy, and high sediment transport capacity. This section is interpreted as a sediment source (erosion-dominated reach). Fine material (silt, very low  $D_{50}$ ) is easily lifted into suspension, and the system is an active supply system. Upstream is the main contributor to suspended sediment. In the midstream section, partial deposition occurs in the middle segment. Meanders slow the local flow, causing sedimentation on the inside of the bend, and the transport capacity begins to decrease. This segment acts as a transition zone (transport and partial deposition). In the downstream section, energy is greatly reduced. Increased deposition occurs, resulting in significant suspended sediment retention and the potential for high siltation. This section functions as a natural sediment trap.

As shown in Figure 5, the upstream section has the highest average flow velocity, and the downstream section has the lowest. Longitudinal sediment analysis shows that the upstream position exhibits high transport. Transport decreases in the middle section, and storage increases in the downstream section (Figure 6). From a flow energy perspective, the sediment is predominantly silt, which is highly sensitive to energy changes. From a system stability perspective, the upstream section exhibits active scour and potential for riverbed degradation. The midstream section exhibits lateral dynamics and local deposition. Meanwhile, the downstream section exhibits dominant aggradation and potential long-term siltation.

For  $D_{50}$  sediment, the  $\tau/\tau_c$  ratio indicates that  $D_{50}$  is always moving. The system is very over-competent against silt.  $D_{50}$  does not determine the stability of riverbed morphology. Morphological changes are more controlled by the coarse fraction ( $D_{90}$ ). The potential for siltation occurs only in the very low energy zone. For the  $D_{90}$  sediment, there is no condition

approaching natural stability. The upstream section has the potential for degradation. The midstream section is very dynamic laterally. The downstream section tends to be a zone of progressive deposition. The system as a whole is not in a static condition, but in active dynamic equilibrium. Table VIII shows the hydraulic and sediment parameters for each segment of the Aur River.

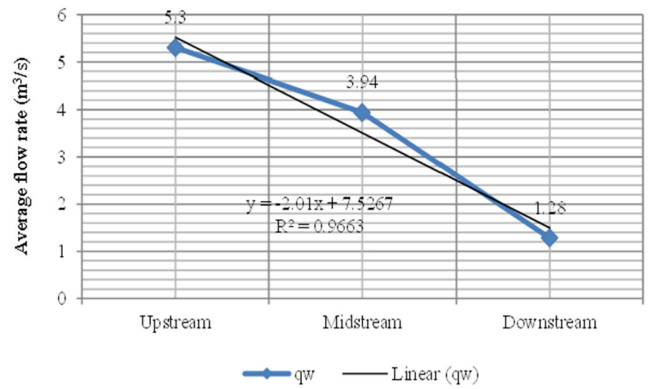


Fig. 5. Average value of flow velocity.

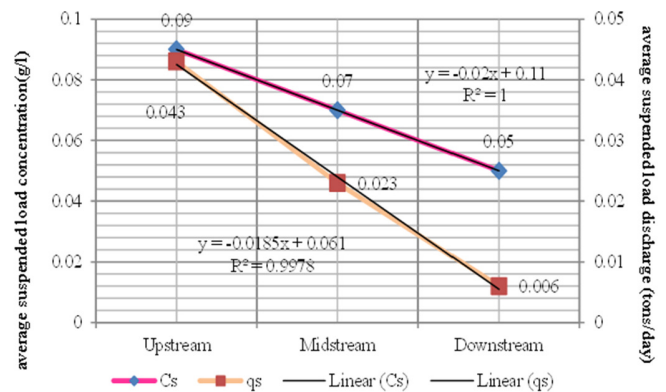


Fig. 6. Average value of sediment concentration and discharge.

According to the results, the Aur River system is currently hydraulically competent to transport fine sediment. Sedimentologically, it is dominated by very fine silt. Morphodynamically, it is dynamically active without an armor layer. Longitudinally, it is experiencing a decrease in energy and sediment supply downstream. Systemically, it is in a supply-limited condition with a tendency toward degradation in the upstream section and relative aggradation in the downstream section.

Table IX shows a significant decrease in both discharge and sediment flow. Sediment  $D_{50}$  tends to increase downstream, and the mobility ratio is very high in all segments.

The analysis results indicate that this river is in a supply-limited condition with a very high level of sediment mobility ( $\tau/\tau_c \gg 1$ ) but produces a relatively low sediment load. Within the framework of the Water Framework Directive, this condition indicates a hydromorphological imbalance, particularly in terms of sediment continuity, which has the

potential to hinder the achievement of good ecological status even though the flow characteristics are still relatively natural.

TABLE VIII. HYDRAULIC AND SEDIMENT PARAMETERS BY THE AUR RIVER SEGMENT

No	Variable	Upstream	Midstream	Downstream	Longitudinal trend
1	Channel width (m)	10.7	11.4	5.8	Narrows downstream
2	Depth (m)	2.3	1.7	1.1	Decreasing
3	Average flow discharge (m <sup>3</sup> /s)	5.30	3.94	1.28	Decreasing
4	Average flow rate (m/s)	0.22	0.20	0.20	Relatively constant
5	D <sub>50</sub> (mm)	0.0156	0.0196	0.0201	Slightly coarsening
6	D <sub>90</sub> (mm)	0.4889	0.3243	0.3445	Fluctuating
7	Shear stress ratio ( $\tau/\tau_c$ ) – D <sub>50</sub>	2975	1927	77.96	Decreasing but >>1
8	Shear stress ratio ( $\tau/\tau_c$ ) – D <sub>90</sub>	94.94	116.49	77.96	Very high mobility
9	Suspended sediment discharge (tons/day)	0.043	0.023	0.006	Sharp decrease

TABLE IX. LONGITUDINAL PERCENTAGE CHANGES BETWEEN SEGMENTS

No	Variable	Upstream to midstream	Midstream to downstream
1	Discharge	-25.7%	-67.5%
2	D <sub>50</sub>	25.6%	2.6%
3	D <sub>90</sub>	-33.7%	6.2%
4	Shear stress ratio ( $\tau/\tau_c$ ) – D <sub>50</sub>	-35.2%	-30.7%
5	Suspended load discharge	-46.5%	-73.9%

IV. CONCLUSIONS

Based on hydraulic and sedimentological analysis, the Aur River is in an active morphodynamic condition with a flow transport capacity that far exceeds the sediment mobilization threshold, both for fine fractions (D<sub>50</sub>) and coarse fractions (D<sub>90</sub>). The very large value of the ratio of shear stress to critical stress ( $\tau/\tau_c$ ) indicates that the river system is over-competent, so that fine sediment is always in suspension and coarse sediment is very easily transported as bed load.

The longitudinal distribution demonstrates a pattern of degradation in the upstream section, dominant transport in the middle section, and a tendency towards aggradation in the downstream section. The non-proportional increase in the discharge-concentration relationship indicates that this system operates in a supply-limited regime, where transport capacity exceeds the available sediment supply. Thus, the long-term stability of the river depends less on changes in flow energy alone, but mostly on changes in sediment supply from the catchment area.

This research provides contextual novelty through a comprehensive study of a local-scale tropical river with specific geomorphological characteristics mapped in detail from upstream to downstream. Unlike previous research, which

generally focuses on large rivers or estuary systems, this study focuses on the morphodynamics of medium-sized rivers dominated by fine sediments during rainy season conditions. This approach yields an empirical understanding of the hydraulic-sedimentological response of tropical rivers to actual increases in discharge in the field.

In terms of methodological novelty, this study simultaneously integrates measurements of rainy season flow velocity, flow discharge, suspended sediment concentration, bed sediment, and grain size distribution analysis (D<sub>50</sub> and D<sub>90</sub>) within a single integrated morphodynamic analysis framework. This integration allows for the identification of system regimes (transport-limited vs. supply-limited), an evaluation of bed stability based on shear stress and Shields parameter approaches, and a sensitivity analysis to discharge changes. This integrated approach provides a more comprehensive quantitative picture than studies that analyze only one component separately.

DECLARATION OF COMPETING INTERESTS

This research was carried out for educational purposes and there are no competing interests.

ACKNOWLEDGMENT

The authors would like to thank the Chancellor of Bina Darma University and the Civil Engineering lecturers at Hasanuddin University, who have helped and supported this learning and research process. This research received no funding.

DATA AVAILABILITY

All originally collected and processed data can be seen within this paper.

REFERENCES

- [1] Rahmawati, M. Tumpu, and A. Yuniarta, "Hydrodynamic and Sedimentological Impacts of Intake Gate Opening Adjustments for Flood Mitigation in Water Systems," *Engineering, Technology & Applied Science Research*, vol. 15, no. 4, pp. 25438–25444, Aug. 2025, <https://doi.org/10.48084/etasr.10729>.
- [2] G. Gladkov, M. Habel, Z. Babiński, and P. Belyakov, "Sediment Transport and Water Flow Resistance in Alluvial River Channels: Modified Model of Transport of Non-Uniform Grain-Size Sediments," *Water*, vol. 13, no. 15, July 2021, Art. no. 2038, <https://doi.org/10.3390/w13152038>.
- [3] G. H. Syamsuddin, M. S. Pallu, F. Maricar, and B. Bakri, "Analysis of the Seasonal Change on the Sediment Transport in the Primary Channel of Saddang Irrigation Area," *Engineering, Technology & Applied Science Research*, vol. 15, no. 1, pp. 20138–20143, Feb. 2025, <https://doi.org/10.48084/etasr.9575>.
- [4] X. Liu, Y. Sun, A. J. Kettner, D. Wang, J. Cheng, and Z. Zou, "Fluvial Sediment Load Characteristics from the Yangtze River to the Sea During Severe Droughts," *Water*, vol. 16, no. 22, Nov. 2024, Art. no. 3319, <https://doi.org/10.3390/w16223319>.
- [5] J. Li, X. Wang, and L. Wu, "Research on Sediment Deposition Characteristics and the Vegetation Restoration of Ecological Riverbanks in the Deep Waterway Regulation Scheme of Yangtze River," *Water*, vol. 16, no. 16, Aug. 2024, Art. no. 2350, <https://doi.org/10.3390/w16162350>.
- [6] A. L. Wildany, R. T. Lopa, and F. Maricar, "Study of Sediment Characteristics in the Jeneberang River's Upstream," *IOP Conference*

- Series: *Earth and Environmental Science*, vol. 1117, 2022, Art. no. 012064, <https://doi.org/10.1088/1755-1315/1117/1/012064>.
- [7] S. N. Devienna *et al.*, "Characterization Of Sedimentary Process In An Estuarine Environment Based On Grain Size Trend Analysis And Geochemical Trace Element In The West Flood Canal River, Semarang," *IOP Conference Series: Earth and Environmental Science*, vol. 1047, 2022, Art. no. 012025, <https://doi.org/10.1088/1755-1315/1047/1/012025>.
- [8] R. D. Putra *et al.*, "Oceanographic conditions and sedimentation in the Kawal river Bintan Island and impact on the prevalence of coral disease," *IOP Conference Series: Earth and Environmental Science*, vol. 1148, 2023, Art. no. 012028, <https://doi.org/10.1088/1755-1315/1148/1/012028>.
- [9] R. A. Rachman, H. D. Armono, M. Wibowo, D. C. Istiyanto, and A. B. Widagdo, "Study of Sediment Distribution in Tanjung Pasir Banten Based on Bed Load Data," *IOP Conference Series: Earth and Environmental Science*, vol. 1224, 2023, Art. no. 012022, <https://doi.org/10.1088/1755-1315/1224/1/012022>.
- [10] A. N. Adilah and M. S. S. Nur Marhidayu, "Study on characteristics of sediment and bed load discharge in Sungai Jemberau at Tasik Chini," *IOP Conference Series: Earth and Environmental Science*, vol. 244, 2019, Art. no. 012046, <https://doi.org/10.1088/1755-1315/244/1/012046>.